S E S 2 0 2 4
Twentieth Anniversary International Scientific Conference
SPACE, ECOLOGY, SAFETY
22 – 25 October 2024, Sofia, Bulgaria

PERIOD REVEALING BY STRUCTURE EMINENCE FUNCTION (SEF). FOUR METHODS. PHOTOMETRIC PERIOD OF ETA CARINAE

Tsvetan Georgiev

Institute of Astronomy and NAO – Bulgarian Academy of Sciences
e-mail: tsgeorg@astro.bas.bg

Keywords: *Time series – periods; Periodograms; LBV stars; Eta Carinae*

Abstract. *SEF is the dependence of the structure amplitude on its time length. The positions of the SEF maxima mark quasi periods and periods. Four methods are distinguished according to their preliminary procedures – with resampling or without resampling of the time series, with local or global detrending. The methods are illustrated on B band data about the LBV η Carinae for the last 60 yr. All methods derive a photometric period of 5.7 ± 0.1 yr, while the known orbital period is 5.54 yr.*

НАМИРАНЕ НА ПЕРИОДИ С ФУНКЦИЯ НА ИЗЯВЕНОСТ НА СТРУКТУРАТА. ЧЕТИРИ МЕТОДА. ФОТОМЕТРИЧЕН ПЕРИОД НА ETA CARINAE.

Цветан Георгиев

Институт по астрономия и НАО – Българска академия на науките
e-mail: tsgeorg@astro.bas.bg

Ключови думи: *Времеви редове – периоди; Периодожреми; LBV Звезди – Eta Carinae*

Резюме: *SEF е зависимостта на амплитудата на структурата от нейната времева дължина. Позициите на максимумите на SEF маркират квази периоди и периоди. Методите се различават според предварителните процедури – със или без ресамплинг на времевия ред, с локален или с глобален детрендинг. Методите са илюстрирани върху B данни за LBV η Carinae за последните 60 г. Всички методи дават фотометричен период 5.7 ± 0.1 г., докато известният орбитален период е 5.54 г.*

Introduction

Various methods for revealing of repetitive structures, responsible for periods in time series or light curves (ICs), exist. In astronomy CLEAN (Roberts, 1987) and Lomb-Scargle (Lomb, 1976; Scargle, 1982) methods, hereafter C&LS, are used.

Our Structure Eminence Function (SEF) is the dependence of the average amplitude of the repetitive structure (pattern) on the structure time length, $E(t_L)$, Eq. 1, Figs.1c – 4c). SEF maxima positions mark quasi periods and periods. We use also a Periodograph Function (PGF), which is derived from the SEF by removal of its background curve, $G(t_L$, Eq. 2, Figs. 1d – 4d). The PGF maxima reveals better the SRF maxima.

The SEF method is tested on various time series. It is compared with the detailed periododgram of Ilkiewicz et al. (2021) about the flickering of AQ Men (Georrgiev 2023, hereafter G23). The SEF method is also applied and compared with C&LC methods on LCs of the LBV η Car (Georgiev et al. 2024, hereafter G+24). Our SEF method reveals and uses average profiles (shapes) of repetitive structures (Fig. 5). By this reason it poses up ro 2 times higher time resolution than the C&CL methods. Also, the structure profiles may be useful in the understanding of the nature of the periodicity.

Four SEF methods may be distinguished, as in Figs. 1 – 4. The subctipts stand for use of resampled (R) or frifinal (O) Lc and applying of local (L) or global (G) detrending.

In Figs. 1&2 SEF_{RL} and SEF_{RG} methods work on an input (ILC) with constant time step. Otherwise, we resample the original LC (OLC) by interpolation with constant time step and derive resampled ILC (RLC). In Figs. 3&4 SEF_{OL} and SEF_{OG} methods work on OLC, without resampling. Eventually, we fill the LC holes by interpolation.

All SEF methods work on flat LCs. i.e. LCs without significant largescale trends. Otherwise, we build a smoothed ILC (SLC) and extract it from the ILC. In Figs. 1&3 SEF_{RL} and SEF_{OL} methods smooth the ILC locally, by moving average. Suitable window size (WS) of the smothing enshre good protrude of the period naximum in the PGF. In Figs. 2&4 SEF_{RG} and SEF_{OG} methods smooth the ILC globally, (G), fitting the ILC with a low degree polynomial.

Further the dependence SEF is building on the residual LC (RLC), which is the difference between the ILC and its SLC. The RLC (Figs. 1b – 4b) has zero average value (AV) and specific standard deviation (SD). The RLC servs all SEF method (Figs. 1c – 4c) and, eventually, C&LS methods (G+24).

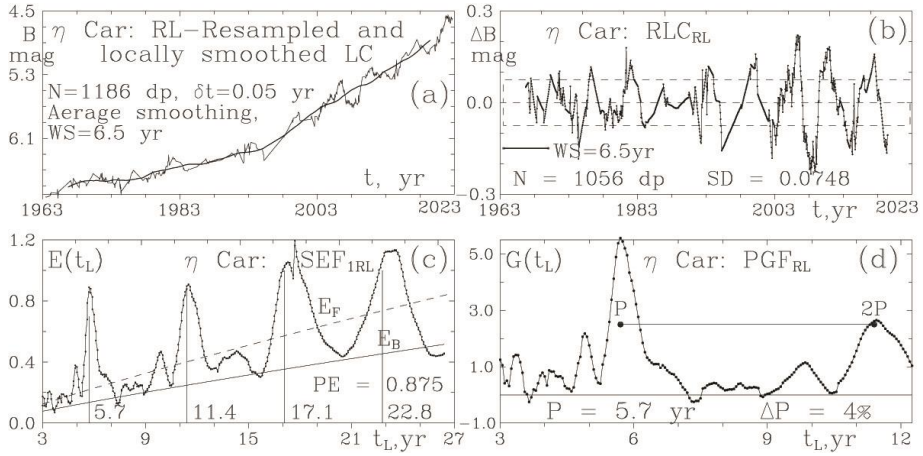

Fig. 1. SEF_{RL} : Resampled LC plus locally detrending through AV from WS of 6.5 yr.

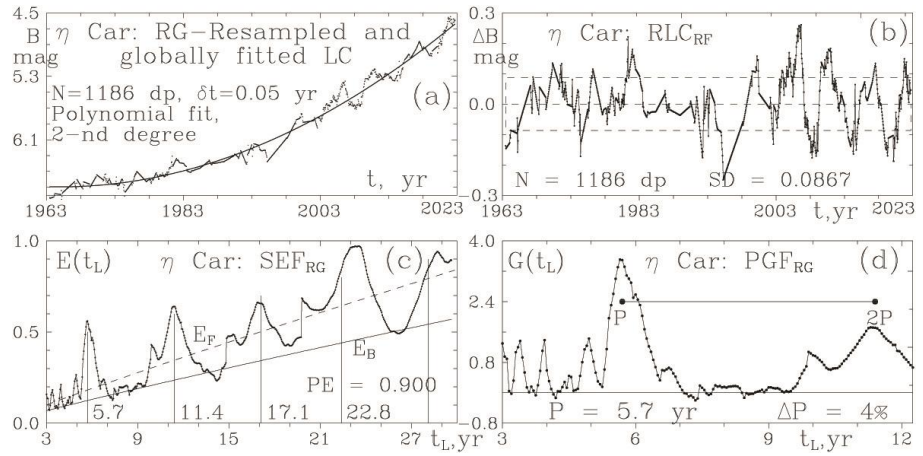

Fig. 2. SEF_{RG} : Resampled LC plus globally detrending through 2-nd degree fit

The used abbreviations follow: AV – average value, C&LC – CLEAN & LC methods, dp – data points, ILC – input LC, LC – light curve, PGF – periodograph function, OLC – original LC, RLC – residual LC, SEF – structure eminence function, SLC – smoothed LC, SD – standard deviation, WS – widow size.

Extracting and characterizing repetitive structures

For methods SEF_{RL} and SEF_{RG} (Figs. 1 & 2) we suppose RLC (t_i, z_i), with i=1,N data points (dp) and constant time step δt. Let this RLC containis a nrepetitive structure with length L dp or time length $t_L=L\times\delta t$. For the extraction of this structure we pull up the first L dp, z_i, i=1,L, from the RLS and put them into an initially empty set with cell numbers j=1, L. Then we add there the next L dp, z_i, $i=L+1,L+L$ from the RLS, after this –the next L dp, etc. The (integer) number of possible additions is

$K=N/L$. In the end the j^{th} cell, containing K additions with respective AV a_j and SD d_j. So, the structure with length L is describing by signal profile a_j and noise profile d_j. Further, the average amplitude $A_L=<|a_{jl}|>_L$ and average noise $D_L=<d_j>_L$ are derived. Note that A_L gathers absolute values $|a_{jl}|$, i.e. A_L is one side average amplitude of the structure. Applying SEF we extract by this manner numerous RLS segments with lengths $L=L_1, L_{max}$, characterizing each of them by A_L and D_L. For at least K=2 additions we have $L_{max}=N/2$.

For the methods SEF_{OL} and SEF_{OG} (Figs. 3 & 4) we have RLC (t_i, z_i) with i=1,N dp, whit arbitrary sampling. Let this RLC contains a repetitive structure with time length t_L.

We extract and add such structures K times, like in the previous case but operating with t_L instead L. Preliminary we derive the left bounds t_{kL}, k=1,K, of numerous intervals, $t_{kL} = t_L \times (k\text{-}1)$. Then we pull up data ($t_i$, z_i) from consecutively RLS segments with time lengths $t_{L\,i}$nto an empty 2D set with N cels. Note, we write time values $t_j = t_i - t_k$ instead t_i. The (integer) number of additions is $K=(t_N\text{-}t_1)/ t_L$. Later we sort the transferred data and derive the sorted data z_j (with suitable shifted times) t_j, representing the profile of the segment with length t_L. Further we resample this multitude data with suitable step. Thus we derive signal profile a_j and noise profile d_j, as well as average amplitude $A_L=<|a_{jl}|>_L$ and average noise $D_L=<d_j>_L$. Applying such SEF method we extract by this manner numerous RLS segments with lengths t_L.

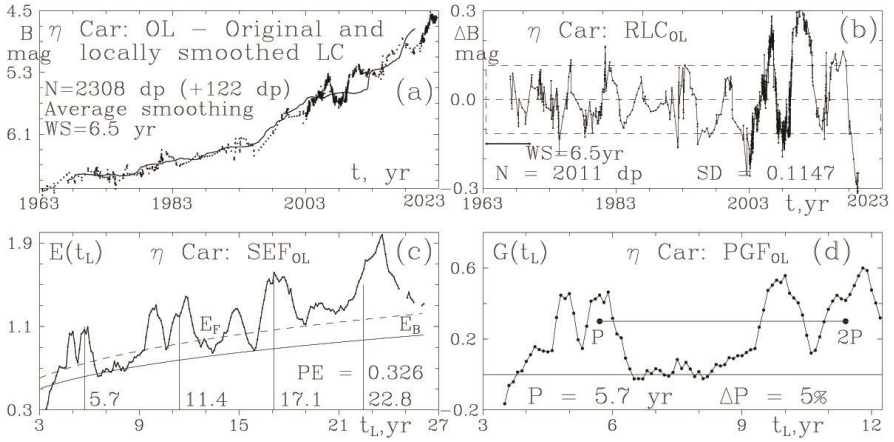

Fig. 3. SEF_{OL}: Original LC plus localy detrending through AV from WS of 6.5 yr.

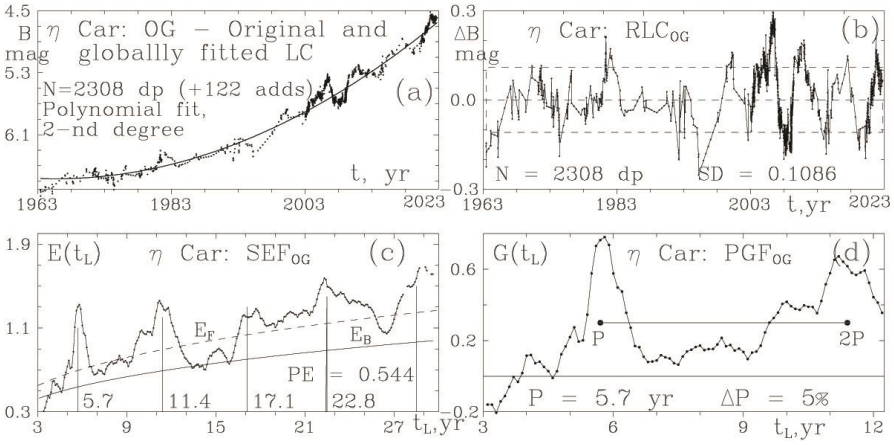

Fig. 4. SEF_{OG}: Original LC plus globally detrending through 2-nd degree fit

Deriving of SEF and PGF

Every significant repetitive structure in the RLC produces maximum of the amplitude funcion A_L and minimum of the noise funcion D_L. Therefore, the ratio A_L / D_L is a good indicator of periods and we define the dimensionless SEF (Figs. 1c – 4c) as follows:

(1) $E_L = A_L / D_L$ or $E(t_L) = A(t_L) / D(t_L)$.

The position of the most left SEF maximum in the SEF marks the basic period P.

The SEF fit, E_F, is a power function (Figs. 1c – 4c, dashed curves). The SEF maxima protrude better above the SEF background. In log-log coordinates the general SEF fit is a lstright ine. Then the background line, which bounds from down 90% of the SEF points, is derived by downward shift of the SEF line. After reverse transform into linear coordinates, the SEF background libe, E_B, becomes power function with the same power exponent (Figs. 1c – 4c, solid curves). So, we define the dimensionless PGF through the SEF values E_L and respective SEF background $E_{L,B}$ (Figs. 1d – 4d,) as follows:

(2) $G_L = (E_L - E_{L,B})/ E_{L,B}$.

The PGF maxima protrude well and the resolution of the SEF method may be estimated better.

Periods from the SEF methods

Figures 1–4 illustrate the applying of the SEF methods on a *B* band LC of LBV *η* Car in 1963–2023, with 2186 dp compilated and homogenized in G+24.

Figures 1a–4a show the ILCs with *N* dp (dots) and the relevant SLCs (curves). In Figs.1a & 2a the ILCs are derived from the OLCs by interpolate resampling with step of 0.05 yr. For Figs. 3a & 4a the step is 0.1 yr, applied after interpolate addition of 122 dp in the holes of the OLC. The maximal hole size is decreased to 0.5 yr. In Figs. 1a & 3a the SLCs are derived from the ILCs by local smoothing with window size WS of 6.5 yr (131 dp), but in Figs. 2a, 4a yhis is performed by 2-nd degree polynomial fit.

Figures 1b–4b show the RLCs, i. e. the differences between the SLC and OLC. The relevant with their *N* and *SD* are implemented. The horizontal lines show the levels “zero” and “zero ±*SD*”. In Figs. 1b & 3b, due to the local smoothing the RLS edges with lengths of 3.25 yr (65 dp) each, are lost. Note, that we use RLC in magnitude difference RLC = –(ILC – LC). So, the positive RLC values correspond to increased brightness.

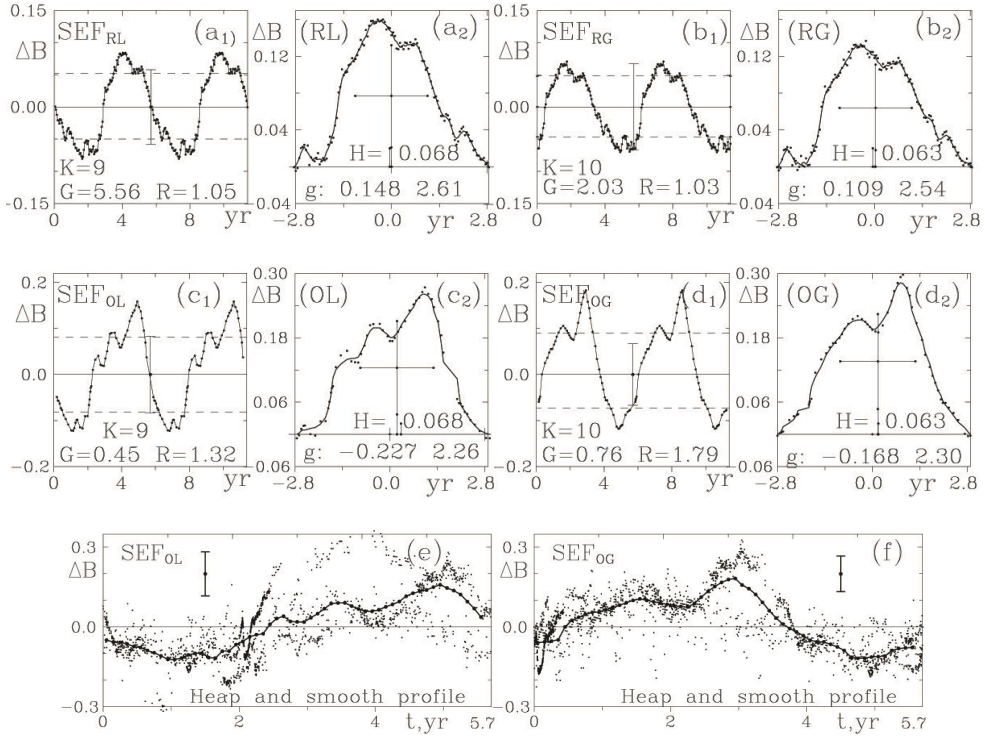

Fig. 5. SEF profiles of the repetitive structures, responsible for the period of 5.7 yr

Figures 1c – 4c show the SEFs, derived from the RLCs (Eq.1, Figs. 1b – 4b). The whole SEFs for *K*=2 cover 27.4 yr (Figs. 1c & 3c) or 29.6 yr (Figs. 2c & 4c). Here E_F and E_B are the power functions of the SEF and SEF s background. respectibelly. PE is the power exponent. The SEF maxima mark the basic period *P* and its default larger counterparts 2*P*, 3*P*, etc. The shorter counterparts, e. g. *P*/2, are not seent.

Figures 1d – 4d show the initial parts of the PGFs (Eq.2). The peaks of the periods *P* and *2P* protrude clearly. The hump resolution isd the the half width at the half of the hump maximum, Δ*t*. For

P=5.7 yr it is 4 - 5% or 0.23 – 0.28 yr. However, the ositions of the hump peaks may be estimated with an accuracy of ±0.1 yr. So, the basic period always is 5.7 ±0.1 yr. The puzzling period at 4.9 ±0.1 yr, protruding in Figs.1 & 3, seems to be a noise appearence.

Profiles of the periods from the SEF methods

Our code may show profiles a_j and d_J, for any repetitive structure, i.e. for any SEF value.

Figures $5a_1$ – $5d_1$ show the average signal profiles, a_j , corresponding to SEF methods in Figs 1—4. Each profile begins from the RLC point No.1, i.e. from an arbitrary phase. This is not an obstacle for deriving the SEF (Eq.1), but for the illustrations here each profile is drawn twice. Vertical bars show the average noise *D* of the profiles, *K* is the number of the profile addins from the RLC, G is the value of the main PGF peak (always at 5.7 yr) and *R* is the ratio between the average heights of the positive, A_1, and negative, A_2, part of the profile. Distances between the edge horizontal lines and the zero level illustrate the values of A_1 and A_2. Note that In Figs.a_1 & b_1 we derive R~1, but In Figs.c_1& d_1 we have R>1. When the positive part is heavy, the profile may be interpreted (somewhat speculative) as product of "flashing".

Figures $5a_2$—$5d_2$ show the shapes of the profiles over their minima. There *H* is the weighted height of this profile and g are the weighted skewness and kurtosis of the shape. Note, that the methods with resampling give profiles with positive skewness, $5a_2$ & $5b_2$. Without resampling the skewness is negative, $5c_2$ & $5d_2$. Note also, that the smooth profiles in $5c_2$ & $5d_2$ are derived with additional smoothing/resampling. Figures.5e & 5f show the original c & d profiles by dots and the respective Smoothed profiles – by curves

Conclusions

Our SEF methods reveal and use average profiles of repetitive structures with a relative resolution of 4–5%, up to 2 times better than the resolution of the C&LS methods. Dependng on the preliminary procedures, the SEF methods have different advantages and disadvantages. In all cases the different data density in the different LC parts may be a problem.

The resampling procedure ensures uniform use of all parts of the RLC. However, many LC peaks may be omitted, which leads to decrease of the peaks in the functions and profiles (Figs. 1, 2, 5a, 5b). Without resampling the time resolution is saved, but the dense part of the RLC will dominates (Figs. 3, 4, 5c, 5d).

The local smoothing by moving AV with suitable WS ensures good protrude of the SEF and PGF peaks, but сш reject the edges of the RLC (Figs. 1, 3). The global smoothing by low degree polynomial fit is a good approach, but it is rarely applicable (Figs.2, 4).

Generally, the methods SEF_{RL} and $SEFO_{OL}$ (Fiigs. 1, 3) seem universal, inspite of the loss of edge RLC data. Note that in Figs. 1 & 3 they reveal an inexplicable period of 4.9 yr.

All methods derive for *η* Car basic period of 5.7 ± 0.1 yr, just like in the study of G+24.

Acknowledgements: The author is grateful to Petko Nedialkov and Antonia Valcheva for the attention and recommendations.

References:

1. Georgiev, Ts. B.: 2023, *Bulg. Astron. J.*, 38, 120–129 [G23]
2. Georgiev, Ts. B., A. Valcheva, P. Nedyalkov, S. Stefanov, M. Moyseev, 2024, *Bulg. Astron. J.*, in print [G+24].
3. Iłkiewicz, K., S.Scaringi, J. M. C. Court, et al.: 2021, *MNRAS,* 503, 4050–4060
4. Lomb, N., R., *Astrophys. & Sp. Sci.*, 1976, 39, 447.
5. Roberts, D., H., J,. Lehar, J. W. Dreher, 1987, *Astron. J.*, 93, 968.
6. Scargle, J., D., 1982, *Astrophis. J*. 263, 835.